Early stage hydration properties of calcium aluminosilicate slag

Y.Y. ZHANG

College of Material Science and Engineering, Chongqing University, Chongqing 400030, P. R. China

Y.H. QI

State Key Laboratory of Advance Steel Processes and Products, Central Iron and Steel Research Institute, Beijing 100081, China

Z.S. ZOU

School of Material and Metallurgy, Northeast University, Shenyang 110819, China

KEYWORD: Calcium aluminosilicate slag; High ferrous bauxite; Hydration properties

ABSTRACT: The calcium aluminosilicate slag cement clinker was prepared from bauxite-coal composite pellets by high temperature reduction and smelting process. The hydration results show that, after hydration for 28 days, the hydration products of calcium aluminosilicate slag are mainly composed of killalaite (Ca3.2(H0.6Si2O7)(OH)), calcium silicate hydrate (Ca1.5SiO3.5 • xH2O) and calcium aluminates hydroxid (3CaO • Al2O3 • Ca(OH)2 • 18 • H2O, Ca12Al13.86Fe0.14(OH)2). With the increase of w(CaO)/w(SiO2) ratio, the killalaite disappeared, the 3CaO • Al2O3 • Ca(OH)2 • 18 • H2O and Ca12Al13.86Fe0.14(OH)2 amounts were increased gradually as a function of w(CaO)/w(SiO2) ratio. The C3A and C12A7 have very exothermic hydration characteristic and faster hydration rate, promoted the hydration activity of β -C2S. The calcium aluminosilicate slag cement clinker has a higher reactivity during the early stage of the hydration process.

INTRODUCTION

Type area

In China, more than 0.5 billion tons of high ferrous bauxite has been explored in the last 20 years (Liu et al. 2012, Wang et al. 2011 & Wang et al. 2010). These high ferrous bauxite is mainly composed of gibbsite ($Al(OH)_3$), diaspore (AlOOH), goethite (FeOOH), hematite (Fe_2O_3) and kaolinite ($Al_2Si_2O_5(OH)4\ 2H_2O$), the content of Al_2O_3 and Fe_2O_3 is over 65wt%, the content of SiO_2 is about 7–12wt% (Liu et al. 2010 & Zhang et al. 2014). Current studies estimate that the coal-based direct reduction method can be used to produce a high quality pig iron from low grade iron ores, and thus it is an ideal technology for adding value to marginal iron ore reserves (Kapure et al. 2011 & Guo et al. 2013). Valuable iron in high ferrous bauxite is preferentially recovered by coal-based direct reduction and melting method (Zhang et al. 2015a). But the residual solid wastes, called calcium aluminosilicate slag, are still discarded as waste in large quantities. However, these calcium aluminosilicate slag with higher Al_2O_3 (28–30%) and CaO (45–55%) content has not been utilized effectively in China. These starting materials lead to a final clinker based on the ternary system $CaO–SiO_2–Al_2O_3$ and are formed by three main minerals: C_2S (dicalcium silicate), $C_{12}A_7$ (mayenite) and C_2AS (gehlenite), other minor phases such as C_3A (tricalcium aluminate), CA (monocalcium aluminate), CA_2 (calcium dialuminate) can also be present (Zhang et al. 2015b).

Conventionally, calcium aluminate cement is produced by fusing limestone as a source of calcium oxide (CaO) and bauxite as a source of aluminium oxide (Al_2O_3) at high temperatures up to 1400℃(Zawrah et al.2011 & David et al. 2013). The chemical composition of calcium aluminate cement may vary over wide range of Al_2O_3 contents ranging between about 40% and 80% (Zawrah et al. 2011). The principal reactive phase is CA and it is responsible for properties of material. Other mineralogical phases appear in minor amounts and C_2S (belite), C_2AS (gehlenite), and ferrite solid solutions, meanwhile the calcium aluminate

cements contain phases such as $C_{12}A_7$, CA, C_3A and CA_2 (Touzo et al. 2001 & Bensted et al, 2002). The $C_{12}A_7$ forms thermodynamically metastable hydrates, such as C_2AH_8, C_4AH_{19}, CAH_{10} etc. at an early hydration time, and then these metastable hydrates convert to thermodynamically stable hydrates such as, C_3AH_6, AH_3 etc (Zhen et al. 2012, Luz et al, 2011 and Pacewska et al. 2013).

It can be seen that the calcium aluminosilicate slag is a kind of clinker which between Portland cement and calcium aluminate cement, has the very high research value. However, as thus to date there have been no comprehensive studies in the pertinent literature on how the calcium aluminosilicate slag systems function.

In this paper, the calcium aluminosilicate slag were synthesized by high temperature reduction and smelting process. The phase composition, microstructure and physical chemical properties of calcium aluminosilicate slag are detected by X-ray diffraction analysis (XRD), scanning electron microscopy (SEM) and energy dispersive microanalysis (EDS). The early hydration mechanical and microstructural properties of calcium aluminosilicate slag were also investigated.

MATERIALS AND METHODS

Synthesis of the calcium aluminosilicate slag

The bauxite powders were thoroughly mixed with anthracite, slaked lime ($Ca(OH)_2$) and fluorite (CaF_2) at different $w(CaO)/w(SiO_2)$ ratios and the mixtures were put into a roller press to compact and produce bauxite-coal composite pellets. Then the bauxite-coal composite pellets were dried at 150℃ for 200 min in a Muffle furnace. After finishing the dried process the bauxite-coal composite pellets were put into a corundum crucible and reduced in a tube furnace at required temperature under N_2 flow rate of 1.5 L/min. After reduction and smelting, the iron nuggets and calcium aluminosilicate slag were magnetic separating. The iron nuggets were used to steel production and calcium aluminosilicate slag was used to produce Portland cement, the whole flow sheet is shown in Fig.1.

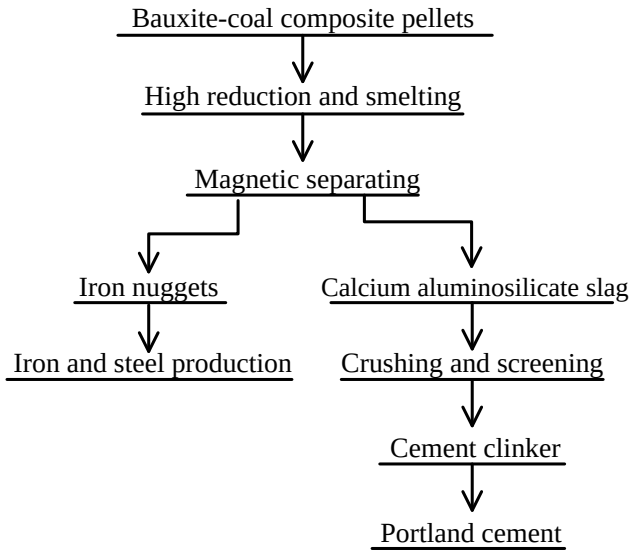

Figure 1. The flow sheet for simultaneously recovering iron and calcium aluminosilicate slag.

Characterization of calcium aluminosilicate slag

The cement clinker of calcium aluminosilicate slag was obtained by crushing, grinding and screening process (see Fig.2). Then it was characterized by using XRD, SEM and EDS to study the phase transformation, morphology and phase composition. The particle size of calcium aluminosilicate slag analysis shows that most of particles are smaller than 120 μm. All samples were dried and sieved to yield a particle size below 74 μm prior to the hydration experiments. The calcium aluminosilicate slag was characterized by using XRD, SEM and EDS to study the phase transformation, morphology and phase composition.

(a) R=3.60, (b) R=3.85, (c) R=4.10

Figure 2. The cement clinker of calcium aluminosilicate slag obtained by crushing and screening.

The chemical compositions of calcium aluminosilicate slag were obtained by XRF and are shown in Table 1. It can be seen that calcium aluminosilicate slag is mainly composed of Al_2O_3, SiO_2 and CaO, the content of Al_2O_3, SiO_2 and CaO is 27.21–29.50wt%, 12.69–13.27wt% and 49.69-53.83wt%, respectively.

Table 1. Chemical compositions of calcium aluminosilicate slag with different w(CaO)/w(SiO_2)

w(CaO)/w(SiO_2)	FeO	Al_2O_3	SiO_2	CaO	MnO	TiO_2	MgO
3.60	3.6	29.5	13.68	49.26	1.34	1.81	0.81
3.85	1.24	28.7	13.29	51.16	2.36	2.42	0.83
4.10	1.33	28.11	13.04	53.48	1.35	1.83	0.86

The effects of w(CaO)/w(SiO_2) ratio on the phase formation of the calcium aluminosilicate slag are shown in Fig. 3. It can be seen that the calcium aluminosilicate slag is mainly composed of calcium silicate, calcium aluminate and gehlenite, with the increase of w(CaO)/w(SiO_2) ratio, the content of gehlenite decreased gradually. When the w(CaO)/w(SiO_2) ratio is 3.60 and 4.10, the β-dicalcium silicate (β-Ca_2SiO_4, β-C_2S), dodecacalcium heptaluminate (12CaO·7Al_2O_3, $C_{12}A_7$) and tricalcium aluminate ($Ca_3Al_2O_6$, C_3A) are the major phases in the calcium aluminosilicate slag, monocalcium aluminate ($CaAl_2O_4$, CA) and gehlenite ($Ca_2Al(Al, Si)_2O_7$, C_2AS) are minor accessories. The phase composition of calcium aluminosilicate slag is listed in Table 2.

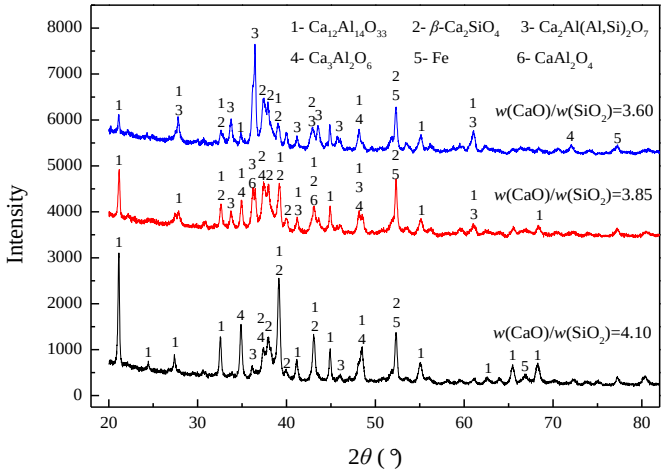

Figure 3. XRD spectrums of calcium aluminosilicate slag with different w(CaO)/w(SiO_2).

Table 2. Mineral components of calcium aluminosilicate slag with different w(CaO)/w(SiO_2)

w(CaO)/w(SiO_2)	βC_2S	$C_{12}A_7$	C_2AS	CA	C_3A	Fe
3.60	26.92	36.54	32.43	-	1.29	2.82
3.85	35.35	44.44	10.27	5.37	3.53	1.04
4.10	25.36	56.79	4.87		7.02	1.09

Hydration mechanism of calcium aluminosilicate slag

The calcium aluminosilicate slag clinkers is mainly composed of β-C_2S, $C_{12}A_7$, C_2AS, CA, C_3A and Fe. The $C_{12}A_7$ and C_3A hydration kinetics are quickly, CA hydration kinetics is relatively slowly, C_2AS does not react with water at room temperature, and β-C_2S phase is hydraulically inactive at early ages. Therefore, all of the hydration reactions are approximately summarized by the following equations (Chotard et al. 2003, Gu et al. 1997, Yang et al. 1984 & Singh 2006):

$$CA + 10H \rightarrow CAH_{10} \quad (1)$$

$$2CA + 11H \rightarrow C_2AH_8 + AH_3 \quad (2)$$

$$3CA + 12H \rightarrow C_3AH_6 + AH_3 \ (T>30℃) \quad (3)$$

$$2C_3A + 27H \rightarrow C_4AH_{19} + C_2AH_8 \quad (4)$$

$$C_3A + CH + 12H \rightarrow C_3AH_{13} \quad (5)$$

$$2C_2S + 4H \rightarrow C_3S_2H_3 + CH \quad (6)$$

$$2\beta\text{-}C_2S + 5H \rightarrow C_3S_2H_4 + CH \quad (7)$$

$$C_{12}A_7 + 53H \rightarrow 6C_2AH_8 + AH_3 + 2CH \quad (8)$$

$$C_{12}A_7 + 51H \rightarrow 6C_2AH_8 + AH_3 \quad (9)$$

$$C_{12}A_7 + 33H \rightarrow 4C_3AH_6 + 3AH_3 \quad (T>30℃) \quad (10)$$

Cement nomenclature is used: C=CaO, A=Al_2O_3, S=SiO_2, H=H_2O, CH=$Ca(OH)_2$, AH_3=$Al(OH)_3$

RESULTS AND DISCUSSION

X-ray diffraction analysis

It is apparent that the w(CaO)/w(SiO_2) ratio is critical to the hydration mechanisms. In order to investigate the effect of w(CaO)/w(SiO_2) ratio on hydration, X-ray diffraction analysis was carried out. Fig. 4 displays the hydratation X-ray patterns of calcium aluminosilicate slag with different w(CaO)/w(SiO_2) ratios after 28 days of hydration. It can be seen that the hydration products are mainly composed of killalaite ($Ca_{3.2}(H_{0.6}Si_2O_7)(OH)$), calcium silicate hydrate ($Ca_{1.5}SiO_{3.5}\cdot xH_2O$, Eq.(7)) and calcium aluminates hydroxid ($3CaO\cdot Al_2O_3\ Ca(OH)_2\cdot 18\ H_2O$, Eq.(4), $Ca_{12}Al_{13.86}Fe_{0.14}(OH)_2$). With the increase of w(CaO)/w(SiO_2) ratio, the main observed transformations were the disappear of killalaite and continuous increase of $3CaO\cdot Al_2O_3\ Ca(OH)_2\cdot 18\ H_2O$ (C_4AH_{19}) and $Ca_{12}Al_{13.86}Fe_{0.14}(OH)_2$ amounts as a function of w(CaO)/w(SiO_2) ratio. As a consequence, the $C_{12}A_7$ and C_3A hydration kinetics are relatively quickly, as expected. On the other hand, C_2AS does not react with water at room temperature, and β-C_2S phase is hydraulically inactive at early ages.

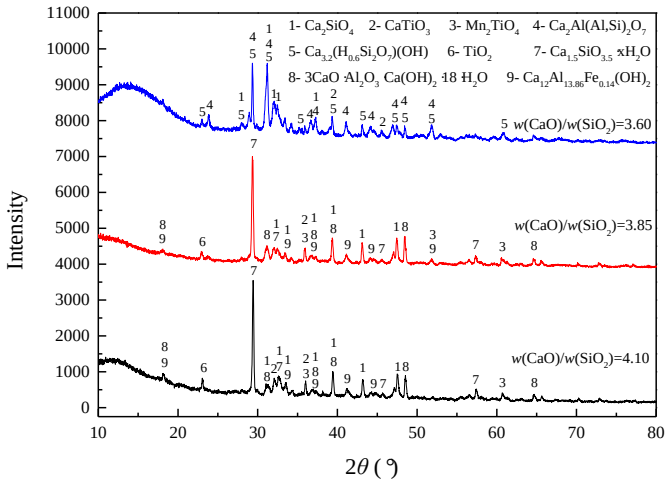

Figure 4. The hydratation XRD patterns of pure C_2S-$C_{12}A_7$ cement material.

Scanning electron microscopy (SEM) analysis

In order to investigate the effect of $w(CaO)/w(SiO_2)$ ratio on hydration microstructure of calcium aluminosilicate slags which were made 28 days after the addition of water. The hydration samples with different $w(CaO)/w(SiO_2)$ ratios were analyzed by SEM and combined the results from the XRD analysis. The SEM photomicrographs and EDS results are displayed in Fig. 5 and Table. 4, respectively. It can be seen that, small crystals are formed in the nanorange with (2-8 μm) different shapes and particle sizes distribution which indicate the formation of heterogeneous materials. This is due to the fast reaction of C_3A and $C_{12}A_7$ with water at early ages of hydration and their very exothermic hydration characteristic. So the formation of stable hydrates occurs sooner ($3CaO\cdot Al_2O_3\ Ca(OH)_2\cdot 18H_2O$, $Ca_{12}Al_{13.86}Fe_{0.14}(OH)_2$). Although β-C_2S is known to react slowly with water in the early stages of hydration, the presence of $C_{12}A_7$ activates β-C_2S and makes it react relatively faster with water than it would do alone. The hydration products of β-C_2S are mainly composed of calcium silicate hydrate ($Ca_{1.5}SiO_{3.5}\ xH_2O$, C–S–H) and $Ca(OH)_2$.

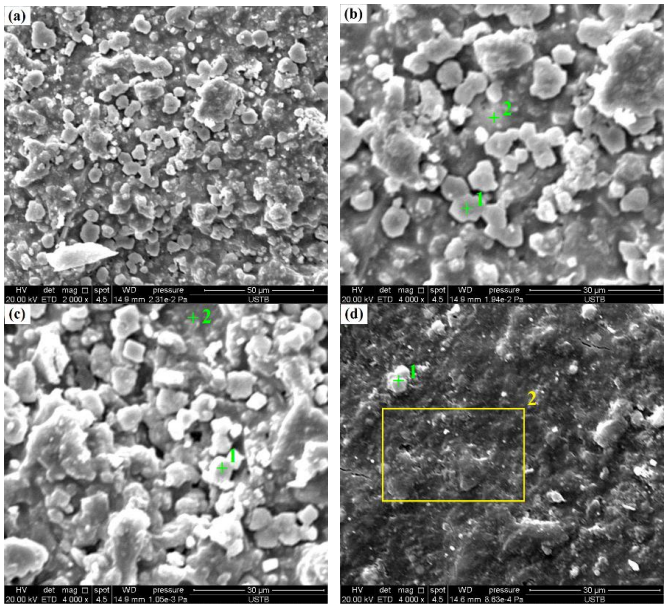

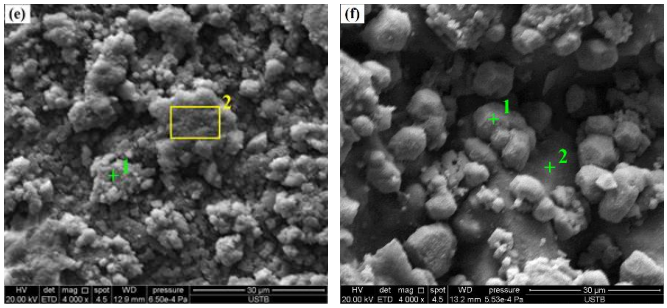

(a)&(b) $w(CaO)/w(SiO_2)$=3.60, (c)&(d) $w(CaO)/w(SiO_2)$=3.85, (e)&(f) $w(CaO)/w(SiO_2)$=4.10
Figure 5. Effects of $w(CaO)/w(SiO_2)$ ratios on hydration microstructure.

Table 4. Analysis results of SEM-EDS

Test positions	Analysis results (at%)						Hydration phase
	C	Si	Al	Ca	O	Sc	
Fig.5 (b)-Spot 1	16.53(2.57 wt%)	-	-	26.42	56.88	0.17	CH
Fig.5 (b)-Spot 2	31.53(3.99 wt%)	4.42	5.03	14.20	44.54	-	C_2AS+CH
Fig.5 (c)-Spot 1	27.51(4.59 wt%)	-	0.04	11.03	61.27	-	C_4AH_{19} + C_2AH_8
Fig.5 (c)-Spot 2	-	3.84	-	35.45	60.11	-	CSH + CH
Fig.5 (d)-Spot 1	18.31(2.67 wt%)	-	0.04	14.35	65.49	-	C_4AH_{19} + C_2AH_8
Fig.5 (d)-Area 2	30.03(4.59 wt%)	1.72	9.2	16.68	42.30	0.07	C_3AH_6 + $3AH_3$
Fig.5 (e)-Spot 1	37.36(3.09 wt%)	-	1.09	12.03	49.52	-	C_3AH_6 + $3AH_3$
Fig.5 (e)-Area 2	16.39(2.54 wt%)	-	-	26.33	56.79	0.15	CH
Fig.5 (f)-Spot 1	27.53(4.59 wt%)	-	0.05	11.08	61.25	-	C_4AH_{19} + C_2AH_8
Fig.5 (f)-Spot 2	30.44(7.17 wt%)	-	7.59	3.37	56.56	-	C_2AH_8 + AH_3

CONCLUSIONS

The calcium aluminosilicate slag cement clinker was prepared from bauxite-coal composite pellets by high temperature reduction and smelting process. The hydration results show that, after hydration for 28 days, the hydration products of calcium aluminosilicate slag are mainly composed of killalaite ($Ca_{3.2}(H_{0.6}Si_2O_7)(OH)$), calcium silicate hydrate ($Ca_{1.5}SiO_{3.5}\cdot xH_2O$) and calcium aluminates hydroxid ($3CaO\cdot Al_2O_3\cdot Ca(OH)_2\cdot 18H_2O$, $Ca_{12}Al_{13.86}Fe_{0.14}(OH)_2$). With the increase of $w(CaO)/w(SiO_2)$ ratio, the killalaite disappeared, the $3CaO\cdot Al_2O_3\cdot Ca(OH)_2\cdot 18\cdot H_2O$ and $Ca_{12}Al_{13.86}Fe_{0.14}(OH)_2$ amounts were increased gradually as a function of $w(CaO)/w(SiO_2)$ ratio. Because the fast reaction of C_3A and $C_{12}A_7$ with water at early ages of hydration and their very exothermic hydration characteristic, the hydration activity of β-C_2S was activated and makes it react relatively faster with water than it would do alone. Therefore, the calcium aluminosilicate slag cement clinker has a higher reactivity during the early stage of the hydration process.

ACKNOWLEDGMENTS

This work was supported by Special Fund for Basic Scientific Research in Colleges and Universities of the Central Business (0903005203413).

REFERENCES

1) Liu, X.F. Wang, Q.F. Zhang, Q.Z. 2012, Mineralogical characteristics of the super large quaternary bauxite deposits in Jingxi and Debao counties, Western Guangxi, China. *Journal of Asian Earth Sciences* 52(3): 53–62.

2) Wang, R.H. Li, M. Chen, D.X. 2011. Resource potential prediction for lateritic high-iron gibbsite bauxite deposits in Guangxi. *Geological Bulletin of China* 30(8): 1303–1311.
3) Wang, Q.F. Deng, J. Liu, X.F. 2010. Discovery of the REE Minerals and its geological significance in the Quyang Bauxite Deposit, West Guangxi, China. *Journal of Asian Earth Sciences* 39(6): 701–712.
4) Liu, X.F. Wang, Q.F. Deng, J. Zhang, Q.Z. Sun, S.L. Meng, J.Y. 2010, Mineralogical and geochemical investigations of the Dajia Salento–type bauxite deposits, western Guangxi, China. *Journal of Geochemical Exploration* 105(3): 137–152.
5) Zhang, Y.Y. Hu, P. Zhang, Z.Y. Qi Y.H. Zou, Z.S. 2014, Mineralogical and geochemical of the guigang Salento-Type bauxite deposits, western guangxi, China. Acta Geodynamica Et Geomaterialia 105(3): 1–7.
6) Kapure, G.U. Rao, C.B. Tathavadkar, V.D. Sen, R. 2011, Direct reduction of low grade chromite overburden for recovery of metals. *Ironmaking & Steelmaking* 38(38): 590–596.
7) Guo, Y.H. Gao, J.J. Xu, H.J. Shi, X.F. 2013, Nuggets Production by Direct Reduction of High Iron Red Mud. *Journal of Iron & Steel Research International* 20(5): 24–27.
8) Zhang, Y.Y. Qi, Y.H. Shi, X.F. 2015, Reduction and Melting Behavior of Carbon Composite Lateritic Bauxite Pellets. *International Journal of Minerals, Metallurgy, and Materials* 22(4): 381–388.
9) Zhang, Y.Y. Shi, X.F. Qi Y.H. Zou, Z.S. 2015, Slag composition mechanism based reduction and smelting of carbon composite bauxite pellets. *Iron and Steel* 50(2): 17–21
10) Zawrah, M.F. Shehata, A.B. Mahmoud, Kishar, E.A. Yamani, R.N. 2011, Synthesis, hydration and sintering of calcium aluminate nanopowder for advanced applications. *Comptes Rendus Chimie* 14(6): 611–618.
11) David, T.M. Lucia, F.C. Sagrario, M.R. 2013, Hydration of calcium aluminates and calcium sulfoaluminate studied by Raman spectroscopy. *Cement & Concrete Research* 47(5): 43–50
12) Touzo, B. Glotter, A. Scrivener, K.L. Mineralogical composition of fondu revisited, in: R.J. Mangabhai, F.P. Glasser (Eds.), [in] *Calcium Aluminate Cements 2001, IOM Communications*, London, 2001: 129–134.
13) Bensted, J. 2002, Calcium aluminate cements, [in] J. Bensted, P. Barnes (Eds.), *Structure and Performance of Cements, 2nd ed., Spon Press*, London: 114-116.
14) Zhen, G.Y. Lu, X.Q. Cheng, B.H. Chen, Yan X.F. Zhao, Y.C. 2012, Hydration process of the aluminate $12CaO \cdot 7Al_2O_3$ assisted Portland cement based solidification/stabilization of sewage sludge. *Construction & Building Materials* 30: 675–681
15) Luz, A.P. Pandolfelli, V.C. 2011, Halting the calcium aluminate cement hydration process. *Ceramics International* 37(8): 3789–3793
16) Pacewska, B. Nowacka, M. Aleknevičius, M. Antonvič, V. 2013, Early Hydration of Calcium Aluminate Cement Blended with Spent FCC Catalyst at Two Temperatures, *Procedia Engineering* 57(1): 844–850.
17) Chotard, T.J. Smith, A. Boncoeur, M.P. 2003, Characterisation of early stage calcium aluminate cement hydration by combination of non-destructive techniques: acoustic emission and X-ray tomography. *Journal of the European Ceramic Society* 23(13): 2211–2223.
18) Gu, P. Beaudoin, J.J. Quinn, E.G. Robert, E. 1997, Early Strength Development and Hydration of Ordinary Portland Cement/Calcium Aluminate Cement Pastes, *Advanced Cement Based Materials* 6(2): 53–58.
19) Yang N.R. Zhong, B.Q. 1984, Ettringite formation and conditions for its stability, *Journal of the Chinese Ceramic Society* 12: 155–159.
20) Singh, N.B. 2006, Hydrothermal synthesis of β-dicalcium silicate (β-Ca_2SiO_4). *Progress in Crystal Growth & Characterization of Materials* 52(1–2): 77–83.